Available online at www.sciencedirect.com
SCIENCE DIRECT®
Physica B 357 (2005) 88–93
PHYSICA B
www.elsevier.com/locate/physb

Using neutron reflectometry and reflection geometry "near-surface" SANS to investigate surfactant micelle organization at a solid–solution interface

W.A. Hamilton[a,*], L. Porcar[a,b,c], L.J. Magid[d]

[a]Center for Neutron Scattering, Condensed Matter Sciences Division, Oak Ridge National Laboratory, Oak Ridge, TN 37831-6393, USA
[b]NIST Center For Neutron Research, Gaithersburg, MD 20899-8562, USA
[c]University of Maryland, MD, USA
[d]Department of Chemistry, University of Tennessee, Knoxville, TN 37996-1600

Abstract

We have used simultaneous neutron reflectometry (NR) and reflection geometry "near-surface" small angle neutron scattering (NS-SANS) to investigate the ordering of cetyltrimethylammonium bromide (CTAB) micelles in aqueous (D_2O) solution in the proximity of a quartz surface as a function of concentration and temperature. The NR measurements allow us to determine coherent micellar organization within a few thousand angstroms of the interface while NS-SANS allows simultaneous monitoring of "bulk" states to the greater depth of grazing incidence penetration into the solution, typically 10–100 μm. We illustrate the utility of this monitoring using the example of an apparent Poiseuille surface shear-induced change in micellar organization which is more probably the result of slight temperature increase.

PACS: 61.12.Ha; 61.12.Ex; 83.80.Qr; 83.85.Hf; 61.30.Hn

Keywords: Neutron reflectometry; SANS; CTAB; Micelles; Poiseuille shear

1. Introduction

It is only to be expected that as the technology of chemical processing achieves capabilities on smaller and smaller length scales and on more complex structured fluids techniques for the monitoring of solution states at interfaces will become increasingly important in guiding the engineering direction of that processing. As is often noted among the techniques which can probe these length scales neutron reflectometry (NR) and small angle [neutron] scattering (SANS) have some

*Corresponding author. Tel.: +1 865 576 6068; fax: +1 865 574 6268.
E-mail address: HamiltonWA@ornl.gov (W.A. Hamilton).

0921-4526/$ - see front matter © 2004 Elsevier B.V. All rights reserved.
doi:10.1016/j.physb.2004.11.028

unique advantages in this regard, since they are: totally non-destructive so measurements may be made on extended time scales; penetrating and therefore sensitive to otherwise obscured or "buried" structures and within a wide variety of sample environment equipment, and with isotopic labelling allowing the enhancement of scattering contrast of or the highlighting of specific substructures within larger molecular aggregations.

In this paper we illustrate the use of NR and simultaneous measurement of "near-surface" SANS (NS-SANS) arising from the beam transmitted beyond a reflecting surface and into its bulk to probe the ordering of cetyltrimethylammonium bromide (CTAB) micelles in solution near a quartz surface—an example which embodies these advantages in the isotropic contrast between the hydrogenous CTAB micelles and their D_2O solvent, and the penetration through 8 cm of crystalline quartz slab to illuminate the solid–solution interface of our reflection geometry cells and of several centimeters of solution to probe the adjacent bulk ordering with NS-SANS.

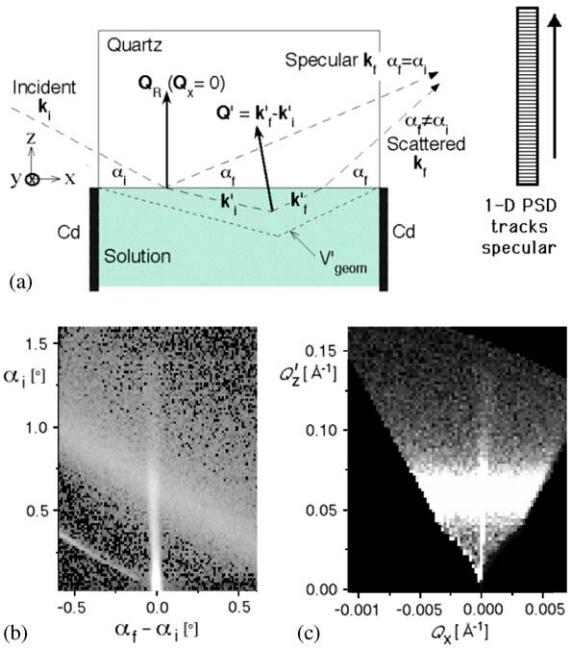

Fig. 1. (a) Schematic of NR/NS-SANS solution cell and measurement geometry. (b) Raw NR/NS-SANS data set 400 mM CTAB in D_2O at 30 °C. (c) Corrected NS-SANS.

2. Experimental

Fig. 1(a) shows the scattering geometry and coordinate definitions used in NR/NS-SANS measurements with our reflection geometry static solution and Poiseuille shear flow cells. The cells used in this measurement have shallow 1 mm deep sample solution troughs meeting a crystal quartz superstrate over a reflecting interface region 8 cm along the beam direction by ~2 cm wide. Poiseuille shear may be applied to a solution simply by pumping it through the trough [1].

NR from this quartz-solution interface probes correlated structures within depths of about 5000 Å into the solution. Our NS-SANS measurements takes advantage of the essentially unavoidable fact that above any critical angle for total reflection most of the neutron beam is transmitted into the solution. SANS within the solution can easily scatter neutrons back towards the surface and towards a downstream detector. In most cases this will be an uncorrelated transport phenomenon—a series of separable events. The transmitted beam, reduced in intensity by 1 minus the reflection coefficient at the interface, is refracted upon crossing the interface, scatters within the solution, and if scattered toward the solution–solid interface is transmitted through it with some probability (by Stokes theorem simply the 1 minus neutron reflectivity we would measure for a beam going the other way—a value available from our NR measurement). The "near-surface" qualifier has been an attempt to distinguish this from the case of "grazing incidence" small angle scattering, which generally assumes some degree of coherent correlation of scattering structures with the surface. At typical grazing incidence angles of ~1° and solution penetration depth of a centimeter or so most NS-SANS occurs at depths ~1–100 μm, well beyond the range of any coherent ordering with respect to the interface.

The corrections for refraction, interfacial transmission and effective sample volume for the simple case of effectively uniform scattering power over the geometrically accessible NS-SANS sample

volume (limited by geometry of refracted incident beam entry and scattered then refracted beam exit from the cell and the total macroscopic cross-section of the solution) required to obtain corrected SANS one-dimensional differential cross-sections with respect to the in-solution scattering vector have been described in detail elsewhere [2].

In the present case as indicated in Fig. 1(a) measurements of specular reflection and off-specular scattering of a 2.59 Å beam were made with the one-dimensional position sensitive detector (PSD) of the Oak Ridge National Laboratory "MIRROR" reflectometer [3] directed along the instrument horizontal reflection plane (the solid-solution reflection interface of our cells was vertical in these measurements). In a NR/NS-SANS scan this detector tracks the reflected beam as the sample is rotated to change the beam angle of incidence to the surface. Thus raw data sets are stacked 1-D PSD images at increasing angle of incidence with the specular signal at a constant position on the detector. Fig. 1(b) shows specular and off-specular scattering for a 400 mM CTAB in D_2O solution at 30 °C in instrument coordinates: angle of grazing specular incidence α_i and the offset (from specular) exit angle $\alpha_f - \alpha_i$. The specular NR signal is seen as vertical stripe at the center of the figure ($\alpha_f - \alpha_i = 0$). Any SANS feature is, of course, at a nearly constant angle to the direct beam. Due to the movement of the detector during the scan this means that these features, in this case a strong NS-SANS signal peak, will cross the data set diagonally. In this scan an edge of the direct beam was allowed to leak past the instrument's direct beam shade and can be seen to be at the same diagonal angle in the lower left-hand corner of the data set.

Fig. 1(c) shows the data corrected for interface transmissions, the effective NS-SANS sample volume and refraction and transformed to reflection plane scattering vector coordinates (Q_x, Q'_z). We now see the NS-SANS peak as a constant feature at an in-solution scattering vector $Q \sim 0.065\,\text{Å}^{-1}$). The procedures for obtaining the NR and absolutely normalized reduced 1-D NS-SANS signals from such MIRROR data sets been described in detail previously [4].

3. Results I: concentration series

Fig. 2(a) shows a series of NR curves and fits for CTAB in D_2O at concentrations of 80, 200, 300, and 400 mM, and pure D_2O. (These NR plots are offset for easy display—a sixth 120 mM CTAB data set is not shown.) Satisfactory fits [5] were obtained for a simple model, shown in Fig. 2(b), of the scattering length density (sld) profile of an absorbed CTAB (sld $= -0.25 \times 10^{-6}\,\text{Å}^{-2}$) layer of ~25 Å thickness and about 85–90% volume fraction, and a decaying oscillation from a nearly pure D_2O sld of $6.3\times10^{-6}\,\text{Å}^{-2}$ just above this layer to a sld consistent with the bulk concentration mix of CTAB in D_2O within 500 Å.

Fig. 2(c) shows fully reduced NS-SANS differential macroscopic scattering cross-sections with respect to scattering vector for this series. The lines following the 80, 200, and 400 mM data points are not fits, but conventional bulk SANS measurements taken using the ORNL 12 m SANS instrument [6] at a wavelength of 4.75 Å. The good agreement indicates the reliability of the NS-SANS reduction procedure in this isotropic scattering case [7]. While fitting this data is beyond the scope of this paper, we note that these curves are essentially consistent with the SANS measurements of

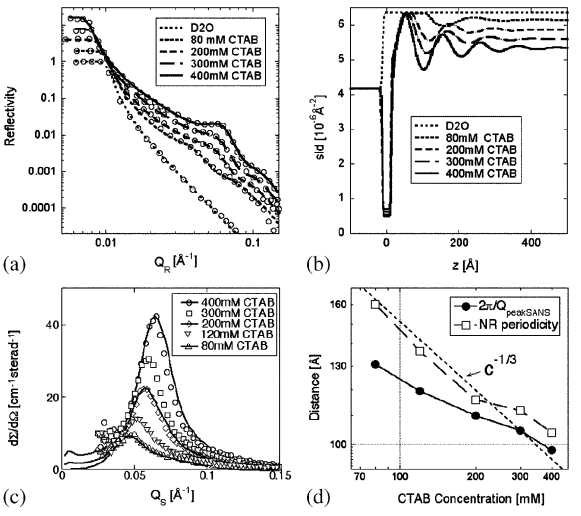

Fig. 2. Concentration series: (a) NR scans—rms resolution approximately indicated by data point width; (b) quartz-solution sld profiles; (c) reduced NS-SANS and bulk SANS data; and (d) characteristic lengths vs. concentration.

Quirion and Magid [8] on this system at 28 °C. Their detailed fits indicated increasingly prolate ellipsoidal micellar aggregation as CTAB concentrations were increased with a maximum aspect ratio of about 2 at their maximum concentration of 300 mM. In our data this is reflected in Fig. 2(d) as we see that both the micellar separation derived from the SANS interaction peak and the layering periodicity at the surface indicated by NR fail to meet the $c^{-1/3}$ behavior expected for constant aggregation number over the concentration range.

It is also interesting to note that over this concentration range the micellar layering periodicity near the surface is greater than the bulk micellar separation, although they do begin to approach the same value at higher concentrations. Further at lower concentrations the layering periodicity does actually follow $c^{-1/3}$ behavior fairly closely. No satisfactory explanation for this observation has occurred to us at this time.

4. Results II: temperature and "shear" series

The original goal of this work was to see if Poiseuille shear-induced surface ordering could be detected in this system at higher concentrations due to either interference between increasingly prolate micelles or simply as a result of hydrodynamic alignment of those few micellar layers nearest the surface probed by NR—previous attempts on more weakly interacting small micelle systems having been generally unsuccessful or inconclusive [9]. In the event we did see a "shear-induced" effect, which as expected was stronger at higher concentrations. However, it is (or should be) a general rule in structural shear measurements to double check that an effect in not just the result of viscous heating—which is also generally, if less interestingly, more pronounced for more concentrated thicker solutions at higher shear rates.

The surface effects of simply heating the solution are illustrated in Fig. 3(a), which shows sld profiles derived from NR measurements on 400 mM CTAB at 30 and 50 °C; the minimum and maximum values of a temperature series covering this range in 5 °C steps. The fits, which use the same model as for the concentration series and are

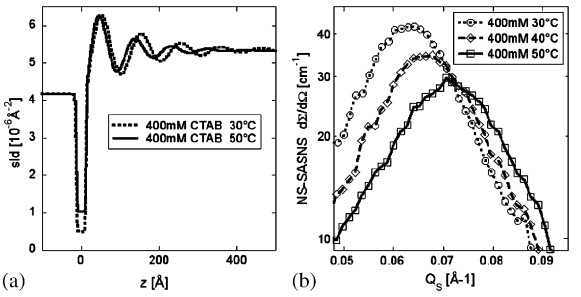

Fig. 3. 400 mM CTAB in D_2O temperature series: (a) sld profiles at 30 and 50 °C, and (b) reduced NS-SANS cross-section at 30, 40, and 50 °C over interaction peak region.

of similar quality to that presented for the 400 mM data in Fig. 2(a), indicate that as the temperature is increased the adsorbed surface layer is to some extent driven from the surface. With an increase in temperature the near surface ordering both decreases in periodicity and by a similar ratio in decay length—over this 20 °C range there is no dramatic change in the correlated layering of micelles with respect to the solid–solution interface. The decrease in periodicity is consistent with the simultaneous NS-SANS measurements for this series shown in Fig. 3(b): as the temperature increases the interaction peak moves to higher scattering vector indicating that the CTAB micelles in the bulk are also becoming closely packed. To maintain constant CTAB concentration this would indicate that the micelle aggregation number and size must also be decreasing.

Analysis of the temperature dependence of the CTAB micelle surface ordering is continuing, however we have been able to apply the results directly as a diagnostic to Poiseuille shear measurements—the NS-SANS results being in effect a monitor of the local bulk solution state within 100 μm of the solid–solution interface. In an attempt to highlight a fairly subtle effect, Fig. 4(a) shows the layering peak region in NR measurements scaled as $R[Q_R]Q_R^4$ versus a 400 mM CTAB solution maintained at a nominal temperature of 35 °C both at rest and at a high applied surface shear rate of about 3000 Hz [10]. Within the resolution and statistical error bars shown the layer peak seems to be narrowing as shear is applied, apparently suggesting what we had hoped

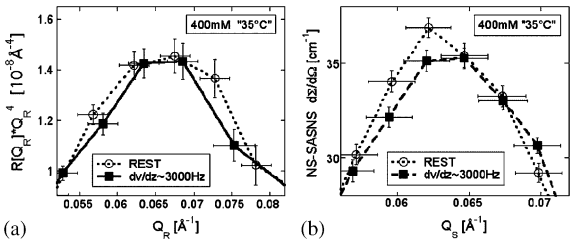

Fig. 4. Temperature/"shear" effects on 400 mM CTAB in D2O at a nominal temperature of 35 °C at rest and at an applied Poiseuille surface shear ~3000 Hz: (a) NR measurement in surface layering peak region scaled as RQ_R^4, and (b) NS-SANS cross-section over the micelle interaction peak region.

to observe: that under Poiseuille flow the prolate micelles near the surface would shear align along the flow direction leading to a more definite surface ordering (and perhaps even surface shear-induced crystallization).

While this might be true, Fig. 4(b) shows that Poiseuille shear is not the only factor at work here. From Fig. 3(b) we saw that over the range 30–50 °C the NS-SANS measured interaction peak position shifts by about 0.0005 $Å^{-1}/°C$, while the peak intensity drops by about 0.7 $cm^{-1}/°C$. Between the runs at rest and at 3000 Hz the rms peak position in Fig. 4(b) moves by about 0.001 $Å^{-1}$ and the peak intensity falls by ~1.5 cm^{-1}. This indicates a temperature increase in the shallow bulk depth probed by NS-SANS of ~2 °C. All the noticeable "shear–induced" changes to NR signals in this series–all on high concentration samples at high shear–showed corresponding temperature increase effects in the simultaneous NS-SANS measurement. Any analysis of the NR data would have the handicap of having to take both effects into account and clearly at these high shear rates our Poiseuille shear cell's temperature control needs to be improved [11] if this is to be avoided in the future.

5. Conclusions

We have presented an outline of the use of NR/NS-SANS to investigate complex fluid structures near a solid–solution interface. Under static (no flow) conditions we have presented some examples of the information which may be derived from these measurements in the case of surface ordering of CTAB micelles in aqueous solution in the proximity of a quartz surface. With respect to the measurement of Poiseuille shear effects on this ordering we have demonstrated how NS-SANS monitoring of the bulk solution may qualify the results of NR measurement. While it is probably true that the present case is a mostly illustrative example and that a temperature sensor placed in the fluid volume closer to the shear cell sample trough would probably have detected the temperature increase we inferred, there are situations for which sensor placement is more difficult: either because of space limitations or disruption of the flow field (for example very thin film high-shear Poiseuille cells [12]), and others for which heating (or, acting similarly, pressure) effects can be expected to be very local: e.g. very viscous solutions and suspensions or granular flows. In such cases we believe NS-SANS monitoring can be a useful diagnostic probe of the "bulk" solution state immediately adjacent to the surface in a Poiseuille sheared fluid.

ORNL is managed by UT-Battelle LLC for the US Department of Energy under contract DE-AC05-00OR22725. We gratefully acknowledge helpful discussions with Dr. Paul Butler (NIST-CNR).

References

[1] Essentially these are smaller versions of the cell we have previously described in detail (S.M.Baker, et al., Rev. Sci. Instrum. 65 (1994) 412), with the modification that the integrated teflon trough has been replaced by an teflon o-ring sealed trough in a stainless steel base.
[2] W.A. Hamilton, et al., Physica B 221 (1996) 309; W.A. Hamilton, et al., Phys. Rev. Lett. 72 (1994) 2219.
[3] W.A. Hamilton, et al., J. Neutron Res. 2 (1994) 1 M. Yethiraj, J.A. Fernandez-Baca, in: D.A. Neuman, T.P. Russell, B.J. Wuensch (Eds.), Materials Research Society Symposium Proceedings 376, "Neutron Scattering in Materials Science II", 1995.
[4] W.A. Hamilton, et al., J. Chem. Phys. 116 (2002) 8533.
[5] The data collection and profile modelling analysis package for MIRROR was developed by W.A. Hamilton and J.B. Hayter. It's NR model fitting uses standard dynamical iterative calculation methods: T.P. Russell, Mater. Sci.

Rep. 5 (1990) 171;
J. Lekner, Physica B 173 (1991) 99.

[6] This instrument has been shortened from the 30 m geometry described in W.C. Koehler, Physica B 137 (1986) 320. Its operation and data correction procedures remain unchanged.

[7] Like most reflectometers MIRROR's transverse (y) resolution is usually relatively poor, in these scans $\delta Q_y = 0.016\,\text{Å}^{-1}$ rms—more than an order of magnitude worse than the instrument's intrinsic perpendicular resolution ($\delta Q_z \sim 0.001\,\text{Å}^{-1}$). However, as δQ_y is by definition the root mean square transverse scattering vector component corresponding to a detector pixel it can, to first order for isotropic scattering, simply be added in quadrature to the in-solution scattering vector on the reflection plane ($Q_y = 0$) to correct for this smearing. This is not an important correction at the Q ranges covered in this work, but would become important at lower Q values or in high-resolution measurements. For details see Ref. [4].

[8] F. Quirion, L.J. Magid, J. Phys. Chem. 90 (1986) 5435.

[9] For example: J. Penfold, et al., Physica B 221 (1996) 325;
M.C. Gerstenberg, et al., Phys. Rev. E 58 (1998) 8028.

[10] Assuming Newtonian parabolic flow profile across the 1 mm trough the applied surface shear rate in Hertz will be numerically equal to 6000 times the mean flow speed through the cell in m/s. So 3000 Hz corresponds to a flow speed of about 0.5 m/s.

[11] In our system the greatest shear rate experienced by a fluid will be in the gear pump driving the flow, thus the most likely place for heating to have occurred. Despite the control and evenness of flow advantages of this pumping system we are currently considering replacing it with peristaltic or a piston driven flow for some applications—including the present one.

[12] T.L. Kuhl, et al., Rev. Sci. Instrum. 72 (2001) 1715.